

## Redox-Active Dithiafulvenyldiphenylphosphine as a Mono- or Bidentate Ligand: Intramolecular Coupling Reaction in the Coordination Sphere of a Metal Carbonyl Fragment

Michel Guerro,<sup>†</sup> Thierry Roisnel,<sup>‡</sup> Pascal Pellon,<sup>†</sup> and Dominique Lorcy<sup>\*†</sup>

Groupe Hétérochimie et Matériaux Electroactifs, SESO UMR 6510 CNRS-Université de Rennes 1, Institut de Chimie de Rennes, Campus de Beaulieu, Bât 10A, 35042 Rennes Cedex, France, and Laboratoire de Chimie du Solide et Inorganique Moléculaire, UMR 6511 CNRS-Université de Rennes 1, Institut de Chimie de Rennes, Campus de Beaulieu, Bât 10B, 35042 Rennes Cedex, France

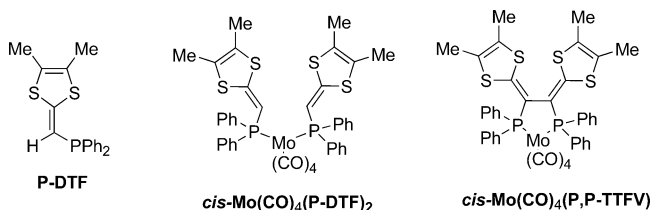
Received January 28, 2005

The coordinating ability of dithiafulvenyldiphenylphosphine (P-DTF) has been investigated with *cis*-W(CO)<sub>4</sub>(piperidine)<sub>2</sub>. As shown by the metal carbonyl complexes obtained, this redox-active vinylphosphine can act as a monodentate (P) and as a bidentate (P,S) ligand. Oxidation of *cis*-M(CO)<sub>4</sub>(P-DTF)<sub>2</sub>, M = Mo and W, leads to the carbon–carbon bond formation between the two coordinated dithiafulvenyldiphenylphosphines. This chemical coupling of the dithiafulvenyl cores in the coordination sphere of M(CO)<sub>4</sub> (M = Mo, W) fragment has been studied in the presence of various oxidizing agents. The use of (BrC<sub>6</sub>H<sub>4</sub>)<sub>3</sub>NSbCl<sub>6</sub> or AgBF<sub>4</sub> induces the formation of a five-membered metallacycle with a vinylous TTF backbone while DDQ leads to a six-membered metallacycle. The syntheses, crystal structures, and electrochemical properties of the complexes obtained are described.

### Introduction

The chemistry of hybrid molecules involving redox-active organic cores such as tetrathiafulvalene (TTF) linked to a metal through a coordination function is currently a topic of great interest.<sup>1–8</sup> The motive power of this research is to create new materials by association and/or interaction of the

organic and inorganic properties in one building block. Various coordination functions have been used to build these hybrid molecules, essentially thiolates,<sup>1</sup> phosphines,<sup>2–5</sup> and pyridines.<sup>6–8</sup> Within this frame, we recently presented a bidentate diphosphine complex with a vinylous tetrathiafulvalene backbone (*cis*-Mo(CO)<sub>4</sub>(P,P-TTFV) which was prepared thanks to an unprecedented metal template effect of molybdenum carbonyl Mo(CO)<sub>4</sub> fragment.<sup>9</sup> Indeed, the two dithiafulvene moieties in Mo(CO)<sub>4</sub>(P-DTF)<sub>2</sub>, *cis* coordinated to the metal via the phosphine, form upon oxidation of the vinylous tetrathiafulvalene core (TTFV) while no coupling reaction was observed for the free uncoordinated vinylphosphine (P-DTF).



Herein, we report the ability of this redox-active vinylphosphine (P-DTF) to also coordinate a tungsten carbonyl W(CO)<sub>4</sub> fragment either as a monodentate (P) or a bidentate

\* Author to whom correspondence should be addressed. E-mail: dominique.lorcy@univ-rennes1.fr. Fax: (33) 2 23 23 67 38.

<sup>†</sup> SESO UMR 6510 CNRS-Université de Rennes 1.

<sup>‡</sup> UMR 6511 CNRS-Université de Rennes 1.

- (1) Kobayashi, A.; Fujiwara, E.; Kobayashi, H. *Chem. Rev.* **2004**, *104*, 5243 and references therein.
- (2) (a) Fourmigué, M.; Batail, P. *Bull. Soc. Chim. Fr.* **1992**, *129*, 29. (b) Fourmigué, M.; Uzelmeier, C. E.; Boubekeur, K.; Bartley, S. L.; Dunbar, K. R. *J. Organomet. Chem.* **1997**, *529*, 343. (c) Uzelmeier, C. E.; Bartley, S. L.; Fourmigué, M.; Rogers, R.; Grandinetti, G.; Dunbar, K. R.; *Inorg. Chem.* **1998**, *37*, 6706. (d) Avarvari, N.; Martin, D.; Fourmigué, M. *J. Organomet. Chem.* **2002**, *643–644*, 292. (e) Devic, T.; Batail, P.; Fourmigué, M.; Avarvari, N. *Inorg. Chem.* **2004**, *43*, 3136. (f) Avarvari, N.; Fourmigué, M. *Chem. Commun.* **2004**, 1300.
- (3) Smucker, B. W.; Dunbar, K. R. *J. Chem. Soc., Dalton Trans.* **2000**, 1309.
- (4) Cerrada, E.; Diaz, C.; Diaz, M. C.; Hursthouse, M. B.; Laguna, M.; Light, M. E. *J. Chem. Soc., Dalton Trans.* **2002**, 1104.
- (5) Pellon, P.; Gachot, G.; Le Bris, J.; Marchin, S.; Carlier, R.; Lorcy, D. *Inorg. Chem.* **2003**, *42*, 2056.
- (6) (a) Iwahori, F.; Gohlen, S.; Ouahab, L.; Carlier, R.; Sutter, J.-P. *Inorg. Chem.* **2001**, *40*, 6541. (b) Setifi, F.; Ouahab, L.; Golhen, S.; Yoshida, Y.; Saito, G. *Inorg. Chem.* **2003**, *42*, 1791.

(P,S) ligand. In our earlier study, we found that the oxidative coupling of *cis*-Mo(CO)<sub>4</sub>(P-DTF)<sub>2</sub> performed in the presence of tris(4-bromophenyl)aminium hexachloroantimonate afforded the metallacycle *cis*-Mo(CO)<sub>4</sub>(P,P-TTFV) in rather low yield.<sup>9</sup> We have therefore explored this chemical coupling of the dithiafulvenyl cores in the coordination sphere of the M(CO)<sub>4</sub> (M = Mo, W) fragment in the presence of various oxidizing agents to improve the overall yield of the oxidation step. Surprisingly, depending on the oxidizing agent used, we can indeed increase the yield of the five-membered metallacycle but also we can favor the formation of a novel six-membered metallacycle. The structural and electrochemical properties of the various complexes obtained are also presented.

## Experimental Section

<sup>1</sup>H NMR and <sup>13</sup>C NMR spectra were recorded on Bruker AC 300P spectrometer. Chemical shifts are reported in ppm referenced to TMS for <sup>1</sup>H NMR and <sup>13</sup>C NMR and to H<sub>3</sub>PO<sub>4</sub> for <sup>31</sup>P NMR. Melting points were measured using a Kofler hot stage apparatus. IR were recorded on Biorad IRFTS 175 C. Elemental analyses results were obtained from the Laboratoire Central de Microanalyse du CNRS, Lyon, France. Mass spectra were recorded with a ZABSpec TOF instrument by the Centre Régional de Mesures Physiques de l'Ouest, Rennes, France. Tetrahydrofuran was distilled from sodium benzophenone. CH<sub>2</sub>Cl<sub>2</sub> was distilled from P<sub>2</sub>O<sub>5</sub>. Toluene was dried over sodium wire. Chromatography was performed using silica gel Merck 60 (70–260 mesh). Mo(CO)<sub>6</sub> and 1,4-diazabicyclo[2.2.2]octane (DABCO) were purchased from ACROS organics. W(CO)<sub>6</sub> was purchased from Aldrich. M(CO)<sub>4</sub>-(NHC<sub>5</sub>H<sub>10</sub>)<sub>2</sub> was prepared from M(CO)<sub>6</sub> according to a published procedure.<sup>10</sup> Cyclic voltammetry was carried out on a 10<sup>-3</sup> M solution of TTF derivatives in dichloromethane containing 0.1 M *n*-Bu<sub>4</sub>NPF<sub>6</sub> as supporting electrolyte. Voltammograms were recorded at 0.1 V s<sup>-1</sup> on a platinum disk electrode (A = 1 mm<sup>2</sup>). The potentials were measured versus the saturated calomel electrode.

**[[4,5-Dimethyl-1,3-dithiol-2-ylidene)methyl]diphenylphosphine-κP]trihydroboron (1).** To a solution of diisopropylamine (1.01 g, 10 mmol) in dry degassed THF (50 mL) was added *n*-BuLi (6.25 mL, 10 mmol, from a 1.6 M solution in hexane) at -20 °C under nitrogen. After the mixture was stirred for 15 min, Ph<sub>2</sub>PMeBH<sub>3</sub> (2.14 g, 10 mmol) in 10 mL of dry THF was added to the medium. The reaction mixture was stirred for an additional 30 min at -20 °C, and 4,5-dimethyl-2-piperidin-1-yl-1,3-dithiol-2-ylum hexafluorophosphate (1.8 g, 5 mmol) was added. The reaction mixture was allowed to reach room temperature and stirred for 4 h. Water was added to the medium (50 mL) and the mixture extracted into 100 mL of CH<sub>2</sub>Cl<sub>2</sub>. The organic phase was washed with water and dried over MgSO<sub>4</sub>, and 20 g of silica gel was added to the solution. After filtration and evaporation of the solvent under reduced pressure, the resulting oil was crystallized by adding diethyl ether to afford **1** as a white powder (820 mg, 48% yield): mp 138 °C; δ<sub>H</sub> (300 MHz; CDCl<sub>3</sub>) 0.6–1.8 (brm, 3H, BH<sub>3</sub>), 1.84 (s, 3H, CH<sub>3</sub>), 1.90 (s, 3H, CH<sub>3</sub>), 5.64 (d, 1H, CH, <sup>2</sup>J<sub>PH</sub> = 7.7 Hz), 7.30–7.75 (m, 10H); δ<sub>P</sub> (121 MHz; CDCl<sub>3</sub>) 14.3 (br m); δ<sub>C</sub> (75 MHz; CDCl<sub>3</sub>) 12.8, 13.5, 91.5 (<sup>1</sup>J<sub>PC</sub> = 65.6 Hz), 122.0, 124.2, 128.8 (<sup>2</sup>J<sub>PC</sub>

= 10.3 Hz), 129.8 (<sup>1</sup>J<sub>PC</sub> = 58.8 Hz), 131.1 (<sup>4</sup>J<sub>PC</sub> = 2.4 Hz), 132.4 (<sup>3</sup>J<sub>PC</sub> = 9.8 Hz), 158.0 (<sup>2</sup>J<sub>PC</sub> = 5.3 Hz). Anal. Calcd for C<sub>18</sub>H<sub>20</sub>BPS<sub>2</sub>: C, 63.17; H, 5.89. Found: C, 63.19; H, 5.93.

**[[4,5-Dimethyl-1,3-dithiol-2-ylidene)methyl]diphenylphosphine (2).** To a solution of **1** (0.64 g, 1.87 mmol) in 40 mL of dry and degassed toluene was added (0.21 g, 1.87 mmol) of DABCO. The medium was heated to 45 °C for 4 h, under nitrogen and the solvent was evaporated. CH<sub>2</sub>Cl<sub>2</sub> was added to the residue, and after filtration on silica gel and evaporation of the solvent, the vinylphosphine **2** was recrystallized in MeOH as a white powder (550 mg, 88%): mp 125 °C; δ<sub>H</sub> (300 MHz; CDCl<sub>3</sub>) 1.91 (s, 3H, CH<sub>3</sub>), 1.92 (s, 3H, CH<sub>3</sub>), 5.90 (d, 1H, CH, <sup>2</sup>J<sub>PH</sub> = 2.3 Hz), 7.2–7.5 (m, 10H); δ<sub>P</sub> (121 MHz; CDCl<sub>3</sub>) -13.2; δ<sub>C</sub> (75 MHz; CDCl<sub>3</sub>) 13.4 (<sup>3</sup>J<sub>PC</sub> = 2.9 Hz), 13.6, 103.6 (<sup>1</sup>J<sub>PC</sub> = 6.8 Hz), 121.1, 122.1 (<sup>4</sup>J<sub>PC</sub> = 8.7 Hz), 128.4, 132.3, 132.5, 138.5 (<sup>1</sup>J<sub>PC</sub> = 7.5 Hz), 152.6 (<sup>2</sup>J<sub>PC</sub> = 40.6 Hz). Anal. Calcd for C<sub>18</sub>H<sub>17</sub>PS<sub>2</sub>: C, 65.83; H, 5.22; S, 19.53. Found: C, 65.80; H, 5.18; S, 19.69.

***cis*-W(CO)<sub>4</sub>(P-DTF)<sub>2</sub> (3) and *cis*-W(CO)<sub>4</sub>(P,S-DTF) (4).** DABCO (0.37 g, 3.3 mmol) was added to a solution of phosphine borane **1** (1.12 g, 3.3 mmol) in 80 mL of degassed toluene, and the reaction mixture was heated to 45 °C for 4 h under nitrogen. *cis*-W(CO)<sub>4</sub>(C<sub>5</sub>H<sub>11</sub>N)<sub>2</sub> (0.76 g, 1.65 mmol) was added to the medium, and after being stirred for 1 h at 45 °C, the solution became homogeneous. The reaction mixture was filtered through celite, which was washed twice with CH<sub>2</sub>Cl<sub>2</sub> (50 mL). The solvent was removed under reduced pressure, and the residue was chromatographed over silica gel (4:2 pentane/ether) affording **3** (692 mg, 65%) and **4** in 29% yield as yellow powders.

***cis*-W(CO)<sub>4</sub>(P-DTF)<sub>2</sub> (3):** mp 184 °C; δ<sub>H</sub> (300 MHz; CDCl<sub>3</sub>) 1.71 (s, 6H, CH<sub>3</sub>), 1.88 (s, 6H, CH<sub>3</sub>), 5.61 (d, 2H, CH, <sup>2</sup>J<sub>PH</sub> = 20.1 Hz), 7.30–7.50 (m, 20H); δ<sub>P</sub> (121 MHz; CDCl<sub>3</sub>) 6.4 (<sup>1</sup>J<sub>PW</sub> = 233 Hz); IR (cm<sup>-1</sup>) ν<sub>C=O</sub> 1867, 1903, 1930, 2013; HRMS (FAB) calcd for C<sub>40</sub>H<sub>34</sub>O<sub>4</sub>P<sub>2</sub>S<sub>4</sub>W 952.032 4, found 952.032 5. Anal. Calcd for C<sub>40</sub>H<sub>34</sub>O<sub>4</sub>P<sub>2</sub>S<sub>4</sub>W: C, 50.43; H, 3.60; S, 13.46. Found: C, 50.61; H, 3.66; S, 13.31.

***cis*-W(CO)<sub>4</sub>(P,S-DTF) (4):** mp 188 °C; δ<sub>H</sub> (300 MHz; CDCl<sub>3</sub>) 2.06 (s, 3H, CH<sub>3</sub>), 2.11 (s, 3H, CH<sub>3</sub>), 6.57 (d, 1H, CH, <sup>2</sup>J<sub>PH</sub> = 2.4 Hz) 7.40–7.60 (m, 10H); δ<sub>P</sub> (121 MHz; CDCl<sub>3</sub>) 52.7 (<sup>1</sup>J<sub>PW</sub> = 237.2 Hz); IR (cm<sup>-1</sup>) ν<sub>C=O</sub> 1869, 1886, 1929, 2016; HRMS (FAB) calcd for C<sub>22</sub>H<sub>17</sub>O<sub>4</sub>PS<sub>2</sub>W 623.981 5, found 623.982 0. Anal. Calcd for C<sub>22</sub>H<sub>17</sub>O<sub>4</sub>PS<sub>2</sub>W: C, 42.32; H, 2.74; S, 10.27. Found: C, 42.38; H, 2.84; S, 10.22.

***cis*-W(CO)<sub>4</sub>(P,P-TTFV) (5).** *cis*-W(CO)<sub>4</sub>(P-DTF)<sub>2</sub> (**3**) (0.29 g, 3 mmol) and (BrC<sub>6</sub>H<sub>4</sub>)<sub>3</sub>NSbCl<sub>6</sub> (0.5 g, 6 mmol) were dissolved in 15 mL of dry degassed CH<sub>2</sub>Cl<sub>2</sub>, and the solution was heated to reflux for 1 h under nitrogen. Na<sub>2</sub>S<sub>2</sub>O<sub>4</sub> (2 g) was added to the medium, and the reaction mixture was stirred under reflux for an additional 1 h. Then the medium was allowed to reach room temperature, washed with water (3 × 10 mL), and dried over Na<sub>2</sub>SO<sub>4</sub>. The solvent was evaporated, and the crude product was purified by chromatography on silica gel using an ether/pentane (1:2) mixture as the eluent to give **5** in 15% yield. Using AgBF<sub>4</sub> as the oxidizing agent, to a solution of **3** (0.13 g, 1.5 mmol) in 10 mL of dry degassed CH<sub>2</sub>Cl<sub>2</sub> was added AgBF<sub>4</sub> (0.05 g, 3 mmol) at 0 °C. The solution was stirred at 0 °C for 2.5 h while the solution turned to dark red, and then Na<sub>2</sub>S<sub>2</sub>O<sub>4</sub> (2 g) was added. After 30 min of stirring, the solution was washed with water (2 × 20 mL) and dried over Na<sub>2</sub>SO<sub>4</sub>. Chromatography over silica gel using an ether/pentane (1:2) mixture as the eluent afforded the desired product in 30% yield: mp 248 °C; δ<sub>H</sub> (300 MHz; CDCl<sub>3</sub>) 1.70 (s, 6H, CH<sub>3</sub>), 2.04 (s, 6H, CH<sub>3</sub>), 7.10–7.90 (m, 20H); δ<sub>P</sub> (121 MHz; CDCl<sub>3</sub>) 41.40 (<sup>1</sup>J<sub>PW</sub> = 226.9 Hz); IR (cm<sup>-1</sup>) ν<sub>C=O</sub> 1859, 1891, 1906, 2009; HRMS (ESI) [M + Na]<sup>+</sup> calcd for C<sub>40</sub>H<sub>32</sub>O<sub>4</sub>NaP<sub>2</sub>S<sub>4</sub>W

(7) Liu, S.-X.; Dolder, S.; Franz, P.; Neels, A.; Stoeckli-Evans, H.; Decurtins, S. *Inorg. Chem.* **2003**, *42*, 4801.

(8) Devic, T.; Avarvari, N.; Batail, P. *Chem.—Eur. J.* **2004**, *10*, 3697.

(9) Lorcy, D.; Guerro, M.; Pellon, P.; Carlier, R. *Chem. Commun.* **2004**, 212.

(10) Darensbourg, D.; Kump, R. L. *Inorg. Chem.* **1978**, *17*, 2680.

Table 1. Crystal Data and Structure Refinement Parameters for 3–6

struct param	3·C <sub>6</sub> H <sub>14</sub>	4	5	6·0.5CH <sub>3</sub> OH
empirical formula	C <sub>46</sub> H <sub>34</sub> O <sub>4</sub> P <sub>2</sub> S <sub>4</sub> W	C <sub>22</sub> H <sub>17</sub> O <sub>4</sub> PS <sub>2</sub> W	C <sub>40</sub> H <sub>32</sub> O <sub>4</sub> P <sub>2</sub> S <sub>4</sub> W	C <sub>40.5</sub> H <sub>34</sub> MoO <sub>4.5</sub> P <sub>2</sub> S <sub>4</sub>
<i>M</i> <sub>r</sub>	1024.76	624.30	950.69	878.8
color	yellow	yellow	orange	yellow
cryst system	triclinic	monoclinic	triclinic	triclinic
space group	<i>P</i> $\bar{1}$	<i>P</i> <sub>2</sub> / <i>c</i>	<i>P</i> $\bar{1}$	<i>P</i> $\bar{1}$
<i>a</i> (Å)	11.814(5)	11.353(5)	11.581(5)	12.361(5)
<i>b</i> (Å)	12.332(5)	10.863(5)	11.885(5)	17.884(5)
<i>c</i> (Å)	15.941(5)	18.796(5)	15.169(5)	19.837(5)
$\alpha$ (deg)	78.860(5)	90	82.590(5)	108.153(5)
$\beta$ (deg)	85.905(5)	100.271(5)	88.004(5)	97.856(5)
$\gamma$ (deg)	74.533(5)	90	70.538(5)	100.075(5)
<i>V</i> (Å <sup>3</sup> )	2195.7(15)	2280.9(16)	1952.1(13)	4016(2)
<i>Z</i>	2	4	2	4
<i>F</i> <sub>000</sub>	1020	1208	944	1796
<i>D</i> <sub>calc</sub> (g/cm <sup>3</sup> )	1.550	1.818	1.617	1.453
$\mu$ (mm <sup>-1</sup> )	2.936	5.343	3.295	0.655
$\theta_{\min}$ , $\theta_{\max}$ (deg)	2.8, 27.52	2.6, 30.0	2.64, 29.99	3.03, 27.5
$\omega$ frame width (deg); time/frame (s)	2; 20	1.6; 48	2; 20	2; 30
tot. no. of measd intensities	18 192	25 197	49 686	59 157
no. of unique data	8860	6507	11 058	16 996
obsd reflns ( <i>I</i> > 2 $\sigma$ ( <i>I</i> ))	6601	4390	6296	9722
no. of refined variables ( <i>n</i> )	515	272	460	939
<i>R</i> <sub>1</sub> ( <i>F</i> ) <sup>a</sup>	0.041	0.031	0.049	0.049
<i>wR</i> <sub>2</sub> ( <i>F</i> ) <sup>b</sup>	0.082	0.0471	0.086	0.0892
GoF <sup>c</sup>	1.030	1.063	1.021	1.027
weighting params <sup>d</sup>	<i>a</i> = 0.0376 <i>b</i> = 3.9852	<i>a</i> = 0.0102 <i>b</i> = 3.2489	<i>a</i> = 0.0308 <i>b</i> = 4.2778	<i>a</i> = 0.0335 <i>b</i> = 7.2812
largest diff map hole and peak (e Å <sup>-3</sup> )	-2.19, 1.512	-1.245, 1.682	-1.423, 1.281	-0.527, 0.56

<sup>a</sup>  $R_1 = \sum_n ||F_o| - |F_c|| / \sum_n |F_o|$  (for  $I > 2\sigma(I)$ ). <sup>b</sup>  $wR_2 = (\sum_n w(F_o^2 - F_c^2)^2 / \sum_n w(F_o^2)^2)^{1/2}$  (for  $I > 2\sigma(I)$ ). <sup>c</sup> GoF =  $(\sum_n w(F_o^2 - F_c^2)^2 / (n - p))^{1/2}$ . <sup>d</sup>  $w = 1/(\sigma^2(F_o^2) + (aP)^2 + bP)$ ;  $P = (\max(F_o^2, 0) + 2F_c^2)/3$ .

973.006 6, found 973.003 4. Anal. Calcd for C<sub>40</sub>H<sub>32</sub>O<sub>4</sub>P<sub>2</sub>S<sub>4</sub>W: C, 50.53; H, 3.39. Found: C, 49.99; H, 3.33.

**Synthesis of Complex 6.** A solution of *cis*-Mo(CO)<sub>4</sub>(P-DTF)<sub>2</sub> (0.5 g, 0.58 mmol) and DDQ (0.35 g, 1.28 mmol) in 25 mL of dry CH<sub>2</sub>Cl<sub>2</sub> was heated to reflux for 30 min under inert atmosphere. Then Na<sub>2</sub>S<sub>2</sub>O<sub>4</sub> was added to the medium. The reaction mixture was washed twice with water, dried over Na<sub>2</sub>SO<sub>4</sub>, and concentrated under reduced pressure. Chromatography over silica gel using an ether/pentane (1/2) mixture as eluent afforded **6** in 43% yield: mp 205 °C;  $\delta_H$  (300 MHz; CDCl<sub>3</sub>) 1.74 (s, 3H, CH<sub>3</sub>), 1.78 (s, 3H, CH<sub>3</sub>), 1.82 (s, 3H, CH<sub>3</sub>), 1.91 (s, 3H, CH<sub>3</sub>), 7.20–8.00 (m, 20H);  $\delta_P$  (121 MHz; CDCl<sub>3</sub>) 44.2 (<sup>2</sup>*J*<sub>PP</sub> = 25 Hz), 56.5 (<sup>2</sup>*J*<sub>PP</sub> = 25 Hz); IR (cm<sup>-1</sup>)  $\nu_{C=O}$  1863, 1901, 1923, 2022; HRMS calcd for C<sub>40</sub>H<sub>32</sub>O<sub>4</sub>P<sub>2</sub>S<sub>4</sub>Mo 863.9712, found 863.9723. Anal. Calcd for C<sub>40</sub>H<sub>32</sub>O<sub>4</sub>P<sub>2</sub>S<sub>4</sub>Mo: C, 55.68; H, 3.74; S, 14.86. Found: C, 55.56; H, 3.81; S, 14.84.

**Synthesis of Complex 7.** A procedure similar to that described above for the molybdenum derivative **6** was used for the synthesis of **7**. Chromatography over silica gel using an ether/pentane (1/2) mixture as eluent afforded **7** in 20% yield: mp 266 °C (dec);  $\delta_H$  (300 MHz; CDCl<sub>3</sub>) 1.74 (s, 3H, CH<sub>3</sub>), 1.78 (s, 3H, CH<sub>3</sub>), 1.83 (s, 3H, CH<sub>3</sub>), 1.92 (s, 3H, CH<sub>3</sub>), 7.10–8.10 (m, 20H);  $\delta_P$  (121 MHz; CDCl<sub>3</sub>) 26.7 (*J*<sub>PP</sub> = 20 Hz, <sup>1</sup>*J*<sub>PW</sub> = 231 Hz), 47.6 (<sup>2</sup>*J*<sub>PP</sub> = 20 Hz, <sup>1</sup>*J*<sub>PW</sub> = 247 Hz); IR (cm<sup>-1</sup>)  $\nu_{C=O}$  1873, 1891, 1909, 2014; HRMS (ESI) [M + Na]<sup>+</sup> calcd for C<sub>40</sub>H<sub>32</sub>O<sub>4</sub>NaP<sub>2</sub>S<sub>4</sub>W 973.006 5, found 973.005 6.

**Single-Crystal Structure Determination.** A single crystal of each compound was carefully selected under a polarizing microscope and glued to a thin fiber glass. Single-crystal data collection was performed at room temperature with a Nonius KappaCCD diffractometer (Centre de Diffractométrie, Université de Rennes, Rennes, France), with Mo K $\alpha$  radiation ( $\lambda = 0.710 73$  Å). A crystal-to-detector distance of 25.0 mm was used for all the crystals, and data collection strategy (determination and optimization of the

goniometer positions) was carried out with the help of the COLLECT program (Nonius, 1998).<sup>11a</sup> Experimental details of the data collection have been summarized in Table 1.

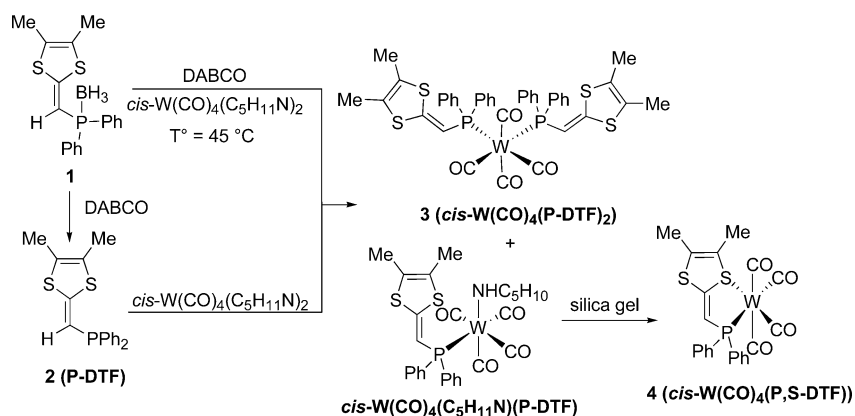
Finally, the integration process and data reduction were carried out using the EVAL program (Duisenberg 1998).<sup>11b</sup> Merging procedure and additional spherical-type absorption correction were applied through the SADABS program (G. Sheldrick, 2002).<sup>12a</sup> Structure determination was performed with the direct methods solving program SIR97 (Altomare, 1999),<sup>11c</sup> which revealed all the non-hydrogen atoms. The SHELXL program (Sheldrick, 1997)<sup>12b</sup> was used to refine the structure. Finally, hydrogen atom were placed geometrically and held in the riding mode in the least-squares refinement procedure. Last cycles of the refinement included atomic positions for all the atoms, anisotropic displacement parameters for all the non-hydrogen atoms, and isotropic displacement parameters for all the hydrogen atoms. Details of the final refinements are given in Table 1 for all compounds.

## Results and Discussion

**Tungsten Complexes of Dithiafulvenyldiphenylphosphine.** The tungsten carbonyl complex of the vinylphosphine (P-DTF) was prepared starting from phosphine borane **1** according to the chemical strategy described in Scheme 1. Decomplexation of this phosphine borane **1** can be realized

- (11) (a) COLLECT: KappaCCD software; Nonius BV: Delft, The Netherlands, 1998. (b) Duisenberg, A. J. M. Reflections on Area detectors. Thesis, Utrecht, The Netherlands, 1998. (c) Altomare A.; Burla M. C.; Camalli M.; Cascarano G.; Giacovazzo C.; Guagliardi A.; Moliterni A. G. G.; Polidori G.; Spagna R. *J. Appl. Crystallogr.* **1999**, *32*, 115–119.
- (12) (a) Sheldrick, G. M. SADABS, version 2.03; Bruker AXS Inc.: Madison, WI, 2002. (b) Sheldrick G. M. SHELX97: Program for the Refinement of Crystal Structures; University of Göttingen: Göttingen, Germany, 1997.

Scheme 1



with DABCO<sup>13</sup> to afford the stable vinylphosphine **2** which can be either isolated or directly used by adding in situ 0.5 equiv of the *cis*-W(CO)<sub>4</sub>(piperidine)<sub>2</sub> complex and heating the medium at 45 °C for 4 h under inert atmosphere. Using these mild conditions, the tungsten complex **3**, *cis*-W(CO)<sub>4</sub>(P-DTF)<sub>2</sub>, was isolated in 63% yield while a 92% yield was obtained for the molybdenum analogue carbonyl complex, *cis*-Mo(CO)<sub>4</sub>(P-DTF)<sub>2</sub>.<sup>9</sup>

Actually, in addition to this complex **3**, we also isolated the monosubstituted tungsten fragment, *cis*-W(CO)<sub>4</sub>(piperidine)(P-DTF), which upon purification by chromatography on silica gel column afforded a yellow crystalline solid. <sup>1</sup>H NMR reveals the disappearance of the piperidino group, and the crystal structure of this complex shows that both the phosphorus and sulfur atoms of the dithiafulvenylphosphine **2** are coordinated to the metal affording the metallacycle **4**, *cis*-W(CO)<sub>4</sub>(P,S-DTF) (Scheme 1 and Figure 1). The removal of the remaining piperidino ligand using

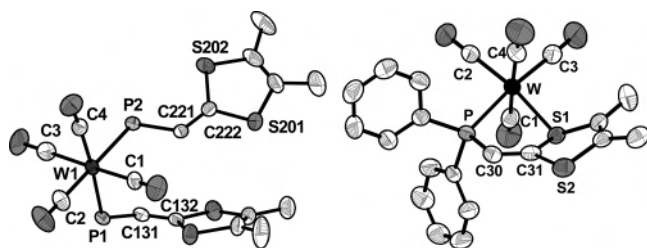


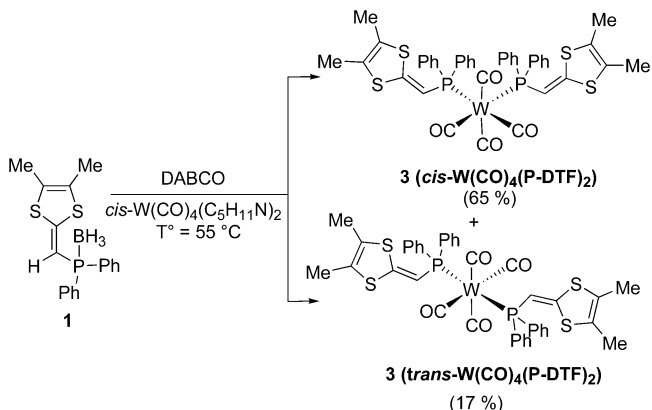
**Figure 1.** Molecular structures of **3**, *cis*-W(CO)<sub>4</sub>(P-DTF)<sub>2</sub> (left), and **4**, *cis*-W(CO)<sub>4</sub>(P,S-DTF) (right), showing the atom labeling (50% probability ellipsoids). Hydrogen atoms and phenyl rings for **3** have been omitted for clarity.

mild acidic conditions, such as a chromatography upon silica gel, is reminiscent of what we previously observed on TTF derivatives.<sup>5</sup> Herein the sulfur atom of the dithiole ring itself, from the already coordinated dithiafulvene **2**, is coordinated to the tungsten, inducing the formation of a five-membered metallacyclic ring, *cis*-W(CO)<sub>4</sub>(P,S-DTF) (**4**). It is noteworthy that the coordination of a dithiole ring through the sulfur atom was rarely encountered.<sup>14</sup> Interestingly, under our reaction conditions, **2** reacted more readily as a mono-

dentate (P) ligand toward *cis*-W(CO)<sub>4</sub>(piperidine)<sub>2</sub> and because of the favorable position of the sulfur toward the resulting free W coordination site left after the departure of the second piperidino ligand, as a bidentate (P,S) one in the formation of the five-membered chelate ring.

To increase the yield of formation of the complex **3**, *cis*-W(CO)<sub>4</sub>(P-DTF)<sub>2</sub>, we modified the experimental procedure by heating the medium at 55 °C instead of 45 °C. We indeed obtained a better yield of the W(CO)<sub>4</sub>(P-DTF)<sub>2</sub> complex (82%), but by increasing the temperature, we also induced the isomerization to the metal center and obtained, besides the *cis*-W(CO)<sub>4</sub>(P-DTF)<sub>2</sub> **3** (65%), the *trans*-W(CO)<sub>4</sub>(P-DTF)<sub>2</sub> **3** (17%) (Scheme 2). The <sup>31</sup>P NMR spectrum of

Scheme 2



the two *cis* and *trans* isomers shows for each one a singlet indicating equivalent phosphorus environments together with a small doublet due to the coupling of the phosphorus atom with the <sup>183</sup>W isotope. The phosphorus atoms resonate at 12.5 ppm with a characteristic <sup>1</sup>J<sub>PW</sub> = 280 Hz for the *trans*-P–W–P isomer and at 6.4 ppm with a <sup>1</sup>J<sub>PW</sub> = 233 Hz for the *cis*-P–W–P one.<sup>15</sup> The *cis* and *trans* configurations are also evident from the <sup>1</sup>H NMR spectrum for the vinylogous proton, which appears as a doublet and resonates at 5.61 ppm (<sup>2</sup>J<sub>PH</sub> = 20 Hz) for the *cis* and 6.38 ppm (<sup>2</sup>J<sub>PH</sub> = 15 Hz) for the *trans*. For our purpose, as only the *cis* isomer can lead to a coupling reaction upon oxidation in the

(13) Brisset, H.; Gourdel, Y.; Pellon, P.; Le Corre, M. *Tetrahedron Lett.* **1993**, *34*, 4523.

(14) Kuroda-Sowa, T.; Hirata, M.; Munakata, M.; Maekawa, M. *Chem. Lett.* **1998**, *27*, 499.

(15) Hirsivaara, L.; Haukka, M.; Pursiainen, J. *Inorg. Chem. Commun.* **2000**, *3*, 508.

**Table 2.** Selected Bond Distances (Å) and Angles (deg) for Compounds 3–5

3, <i>cis</i> -W(CO) <sub>4</sub> (P-DTF) <sub>2</sub>		4, <i>cis</i> -W(CO) <sub>4</sub> (P,S-DTF)		5, <i>cis</i> -W(CO) <sub>4</sub> (P,P-TTFV)	
W1–C2	1.975(6)			W1–C1	1.986(7)
W1–C4	1.994(6)	W–C2	1.974(4)	W1–C3	1.991(6)
W1–C3	2.029(6)	W–C3	1.982(5)	W1–C4	2.026(8)
W1–C1	2.031(6)	W–C4	2.024(5)	W1–C2	2.028(8)
W1–P1	2.5419(16)	W–C1	2.037(5)	W1–P1	2.4814(16)
W1–P2	2.5486(16)	W–S1	2.4992(12)	W1–P2	2.5033(16)
P1–C131	1.807(5)	W–P	2.5068(12)	P1–C131	1.835(5)
P2–C221	1.788(5)	P–C30	1.808(4)	P2–C231	1.828(5)
C131–C132	1.340(7)	C30–C31	1.328(5)	C131–C132	1.376(7)
C221–C222	1.346(7)	S1–C31	1.785(4)	C131–C231	1.477(7)
S201–C222	1.752(5)	S2–C31	1.748(4)	C231–C232	1.378(7)
S202–C222	1.745(5)			S3–C232	1.759(5)
				S4–C232	1.755(5)
P1–W1–P2	91.25(5)	S1–W–P	76.51(3)	P1–W1–P2	79.23(6)
C131–P1–W1	119.02(17)	C30–P–W	106.72(13)	C131–P1–W1	110.21(17)
C221–P2–W1	113.88(17)	C31–S1–W	105.70(13)	C231–P2–W1	107.70(17)
C132–C131–P1	123.2(4)	C31–C30–P	118.3(3)	C132–C131–C231	121.4(5)
C222–C221–P2	128.6(4)	C30–C31–S2	128.9(3)	C132–C131–P1	121.1(4)
C221–C222–S202	126.1(4)	C30–C31–S1	120.6(3)	C231–C131–P1	116.7(4)
C221–C222–S201	122.0(4)	S2–C31–S1	110.6(2)	C232–C231–C131	121.2(5)
S202–C222–S201	111.9(3)			C232–C231–P2	125.2(4)
				C131–C231–P2	113.4(4)
				C231–C232–S4	126.3(4)
				C231–C232–S3	122.5(4)
				S4–C232–S3	111.2(3)

coordination sphere of the M(CO)<sub>4</sub> fragment, we did not pursue in the optimization of the **3** *cis* isomer formation. The complexes **3**, *cis*-W(CO)<sub>4</sub>(P-DTF)<sub>2</sub>, and **4**, *cis*-W(CO)<sub>4</sub>(P,S-DTF), were crystallized in MeOH.

The X-ray crystal structure of **3** and **4** are shown in Figure 1, and selected bond distances and angles are listed in Table 2. Within the complex **3**, the two dithiafulvene moieties are *cis* coordinated to the metal center via the phosphorus atom. Phosphorus–tungsten bond lengths are in the usual range (W1–P1 2.5419(16) and W1–P2 2.5486(16) Å) with a P1–W–P2 interligand angle of 91.25(5)°. Each dithiole ring is planar with a distance between the two carbons involved in the coupling reaction for the formation of the vinylogous TTF backbone of about 3.78 Å. Concerning complex **4**, the tungsten center is surrounded by the *cis*-coordinated P,S-ligand **2**; the W–P and W–S distances (W–S1 2.4992(12) and W–P 2.5068(12) Å) are as expected with a bite angle of S–W–P 76.51(3)°. As seen in Figure 1, the five-membered ring is not planar and adopts an envelop conformation with the tungsten atom above the plane formed by the P–C=C–S fragment; moreover, the dithiole ring is not planar and the folding along the S···S axis reaches a value of 27°. This folding of the dithiole ring is induced by the metallacycle as for instance in *cis*-W(CO)<sub>4</sub>(P-DTF)<sub>2</sub> (**3**) the two dithiole rings are planar. This can be observed in Figure 1b representing the molecular structure of **4**. Coordination through the sulfur atom introduces also a dissymmetry in the dithiole ring of **4** with a lengthening of the metallacycle C–S bond (S1–C31 1.785(4) Å) while the other C–S bond is in the usual range (S2–C31 1.748(4) Å).

The redox behavior of **3** and **4** was investigated by cyclic voltammetry, and the data are collected in Table 3 together

**Table 3.** <sup>31</sup>P NMR Spectroscopic Data and Oxidation Peak Potentials in V vs SCE for 2–5

compd	δ( <sup>31</sup> P), ppm	E <sub>pa</sub> <sup>1</sup>	E <sub>pa</sub> <sup>2</sup>
<b>2</b> <sup>9</sup>	–13.2	0.73 <sup>a</sup>	
<i>cis</i> -Mo(CO) <sub>4</sub> (P-DTF) <sub>2</sub> <sup>9</sup>	24.1	0.60 <sup>a</sup>	1.35 <sup>a</sup>
<b>3</b> , <i>cis</i> -W(CO) <sub>4</sub> (P-DTF) <sub>2</sub>	6.7	0.65 <sup>a</sup>	1.35 <sup>a</sup>
<b>4</b> , <i>cis</i> -W(CO) <sub>4</sub> (P,S-DTF)	52.7	0.97 <sup>a</sup>	1.57 <sup>a</sup>
<i>cis</i> -Mo(CO) <sub>4</sub> (P,P-TTFV) <sup>9</sup>	56.9	0.48	1.25 <sup>a</sup>
<b>5</b> , <i>cis</i> -W(CO) <sub>4</sub> (P,P-TTFV)	41.4	0.49	1.29 <sup>a</sup>

<sup>a</sup> Irreversible process.

with those for **2** and *cis*-Mo(CO)<sub>4</sub>(P-DTF)<sub>2</sub> for comparison. For **3** and **4**, two irreversible oxidation waves are observed assigned in both cases for the first one to the oxidation of the dithiafulvene core into the cation radical and for the second one to the oxidation of the metallic center. It is worth noting that depending on the coordination mode either as a monodentate (P) in **3** or as a bidentate (P,S) ligand in **4**, the oxidation peak potential for the dithiafulvene moiety is significantly affected. Indeed, a positive shift of 320 mV is observed when the dithiole ring is also coordinated through the sulfur atom to the tungsten carbonyl fragment, *cis*-W(CO)<sub>4</sub>(P,S-DTF), which exerts an electron-withdrawing influence. Contrariwise, and as already observed for *cis*-Mo(CO)<sub>4</sub>(P-DTF)<sub>2</sub>,<sup>9</sup> the oxidation peak potential for **3** is at a lower potential than the vinylphosphine ligand **2** itself indicating this time an electron-donating effect of the metallic center on the dithiafulvene.

**Oxidation Studies of the Complexes *cis*-M(CO)<sub>4</sub>(P-DTF)<sub>2</sub>.** The oxidative coupling of the dithiafulvene moieties *cis*-coordinated to the metal center in complexes *cis*-M(CO)<sub>4</sub>(P-DTF)<sub>2</sub> (M = Mo, W) was investigated in the presence of various oxidizing agents. As shown recently for the molybdenum derivative, chemical oxidation performed with tris(4-bromophenyl)aminium hexachloroantimonate, (BrC<sub>6</sub>H<sub>4</sub>)<sub>3</sub>NSbCl<sub>6</sub>,<sup>17</sup> induced the formation of the bidentate diphosphine complex with a redox-active vinylogous TTF

(16) Hirsivaara, L.; Haukka, M.; Jääskeläinen, S.; Laitinen, R. H.; Niskanen, E.; Pakkanen, T. A.; Pursiainen, J. *J. Organomet. Chem.* **1999**, 579, 45.

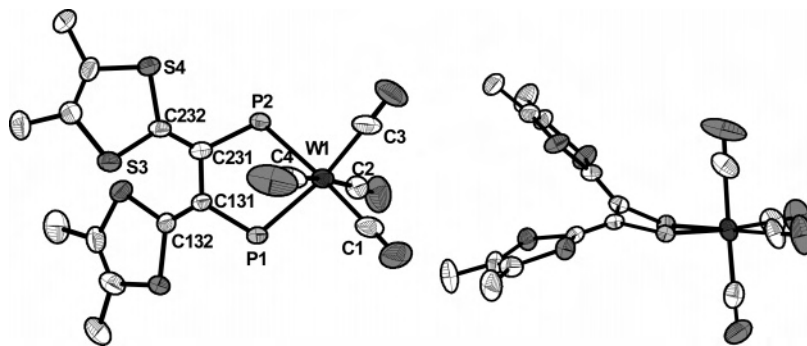
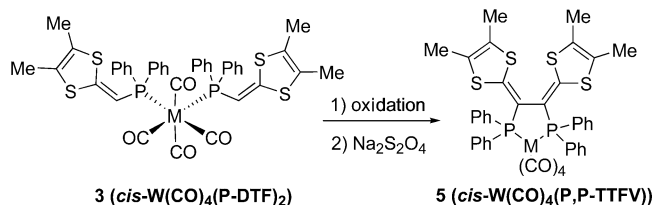


**Figure 2.** Molecular structures of **5**, *cis*-W(CO)<sub>4</sub>(P,P-TTFV), showing the atom labeling (left) and the distorted conformation of the metallacycle (right) (50% probability ellipsoids). Hydrogen atoms and phenyl rings have been omitted for clarity.

### Scheme 3

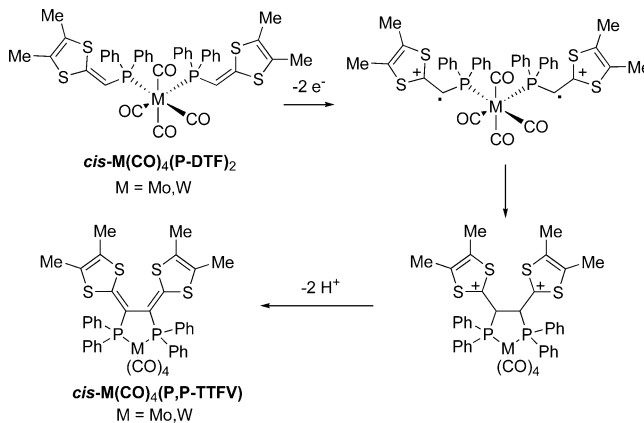


backbone (Scheme 3).<sup>9</sup> Thus, the coupling reaction of **3** (*cis*-W(CO)<sub>4</sub>(P-DTF)<sub>2</sub>) was performed under the same conditions with 2 equiv of (BrC<sub>6</sub>H<sub>4</sub>)<sub>3</sub>NSbCl<sub>6</sub> in dichloromethane under inert atmosphere at reflux for 1 h followed by the reduction with Na<sub>2</sub>S<sub>2</sub>O<sub>4</sub> (Scheme 3).

The intramolecular C–C bond formation between the two dithiafulvene rings also occurs affording the metallacycle **5**, *cis*-W(CO)<sub>4</sub>(P,P-TTFV). As previously demonstrated, the oxidative coupling of 1,4-dithiafulvenes proceeds through a radical cation–radical cation mechanism.<sup>18</sup> Therefore, we can postulate that the formation of the metallacycle occurs according to a similar mechanism: (i) oxidation of the *cis*-M(CO)<sub>4</sub>(P-DTF)<sub>2</sub> by (BrC<sub>6</sub>H<sub>4</sub>)<sub>3</sub>NSbCl<sub>6</sub> into a bis radical cation; (ii) coupling of the bis radical cation; (iii) deprotonation of the intermediate to afford the vinylogous TTF core (Scheme 4). In the medium the vinylogous TTF is oxidized to the dication, which is further reduced by sodium hydro-sulfite. The <sup>31</sup>P NMR spectrum of **5** in CDCl<sub>3</sub> shows one signal at δ 41.40 ppm indicating that the two P atoms are in the same chemical environment. Moreover, the phosphorus atoms resonate at lower field than in the noncyclic complex **3** and a deshielding of 35 ppm is observed indicating a great degree of steric strain in accordance with the formation of a five-membered ring.<sup>19</sup> Similarly, a deshielding of 32.8 ppm was observed for the molybdenum metallacycle *cis*-Mo(CO)<sub>4</sub>(P,P-TTFV).<sup>9</sup>

The crystal structure confirmed the formation of a metallacycle resulting from intramolecular carbon–carbon bond formation upon oxidation. The X-ray molecular structure of

### Scheme 4



**5** is shown in Figure 2, and selected bond distances and angles are listed in Table 2. As previously observed for the molybdenum derivative, the five-membered ring is not planar and adopts a half-chair conformation. This distorted conformation is due to the steric strains generated by the two planar dithiole rings with an acute dihedral angle based on the central C–C bond between the two dithiole rings of 48.77° and the shortest S···S contact between the sulfur atoms of the two dithiole rings of 3.12 Å. Comparison of the bond lengths within this metallacycle **5** and the starting complex **3** shows that the intramolecular cyclization causes some changes notably in the phosphorus–tungsten distances which are shortened (W1–P1 2.4814(16) and W1–P2 2.5043(16) Å), and the P–C bonds are slightly longer with

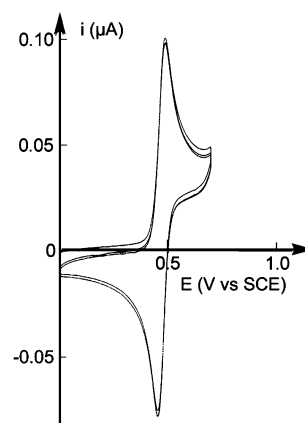


**Figure 3.** Cyclic voltammetry of *cis*-W(CO)<sub>4</sub>(P,P-TTFV) in CH<sub>2</sub>Cl<sub>2</sub>–0.1 M NBu<sub>4</sub>PF<sub>6</sub> (scan rate 0.1 V s<sup>-1</sup>).

- (17) (a) Ohta, A.; Yamashita, Y. *J. Chem. Soc., Chem. Commun.* **1995**, 1761. (b) Yamashita, Y.; Tomura, M.; Braduz Zaman, M.; Imaeda, K. *J. Chem. Soc., Chem. Commun.* **1998**, 1657. (c) Yamashita, Y.; Tomura, M.; Imaeda, K. *Tetrahedron Lett.* **2001**, 42, 4191. (d) Yamashita, Y.; Tomura, M. *J. Solid State Chem.* **2002**, 168, 427.
- (18) (a) Hapiot, P.; Lorcy, D.; Carlier, R.; Tallec, A.; Robert, A. *J. Phys. Chem.* **1996**, 100, 14823. (b) Guerro, M.; Carlier, R.; Lorcy, D.; Hapiot, P. *J. Am. Chem. Soc.* **2003**, 125, 3159.
- (19) Garrou, P. E. *Inorg. Chem.* **1975**, 14, 1435.

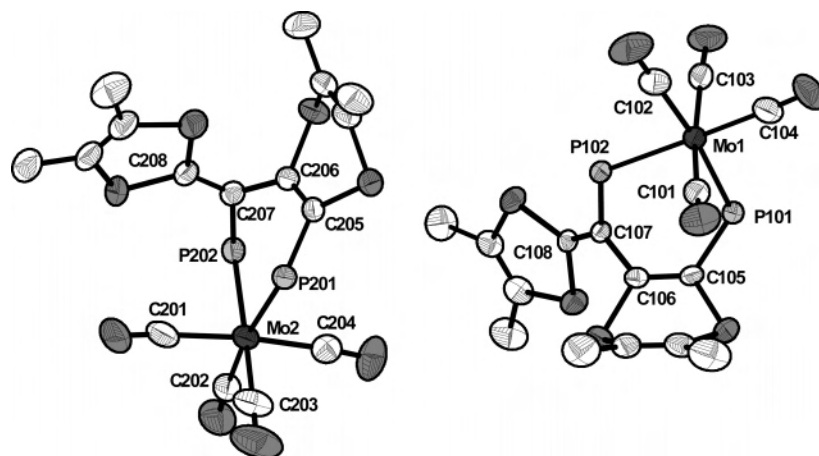
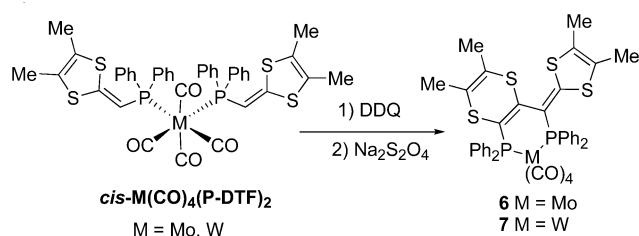


**Figure 4.** Molecular structures of **6** showing the two different molecules **A** (right) and **B** (left) and the atom labeling (50% probability ellipsoids). Hydrogen atoms and phenyl rings have been omitted for clarity.

### Scheme 5



a P1–W–P2 interligand angle of  $79.23(6)^\circ$ . Among the spacer group between the two dithiole rings, the C=C bonds are longer than in either nonsubstituted or substituted vinyllogous TTF.<sup>20</sup>

The redox behavior of *cis*-M(CO)<sub>4</sub>(P,P-TTFV), M = Mo<sup>9</sup> and W, was investigated by cyclic voltammetry, and the data are collected in Table 3. For the two complexes two oxidation waves were observed. The first is reversible and bielectronic and corresponds to the oxidation of the vinyllogous TTF core into the dication (Figure 3), while the second one is irreversible and attributable to the oxidation of the metallic center. The nature of the metallic center does not modify the oxidation potential of the TTFV core (e.g.  $E = 0.48$  V for Mo and  $E = 0.49$  V for W). The redox behavior of the vinyllogous TTF core in these complexes is closely related to what was observed for other constrained TTFV's either when the central conjugation of the vinyllogous TTF is part of a six-membered ring<sup>17a</sup> or when there are cyclophane-like vinyllogous TTFs, with a short aliphatic link connecting the two dithiole rings imposing a similar geometry.<sup>18b</sup> Indeed, in all these cases, the presence of steric strain (either by the link or here by complexation) leads to the concomitant exchange of two electrons. Another salient feature of vinyllogous TTF concerns the molecular movements associated with the electron transfer;<sup>17b,18b,20</sup> one expects therefore that oxidation of *cis*-M(CO)<sub>4</sub>(P,P-TTFV) would induce similar conformational changes due to the presence of the metallacycle.

We also investigated the coupling reaction of *cis*-M(CO)<sub>4</sub>(P-DTF)<sub>2</sub> (M = Mo, W) in the presence of other oxidizing agents. For instance we replaced (BrC<sub>6</sub>H<sub>4</sub>)<sub>3</sub>NSbCl<sub>6</sub> first by iodine which was known for inducing a similar coupling

**Table 4.** Selected Bond Lengths (Å) and Angles (deg) for **6**

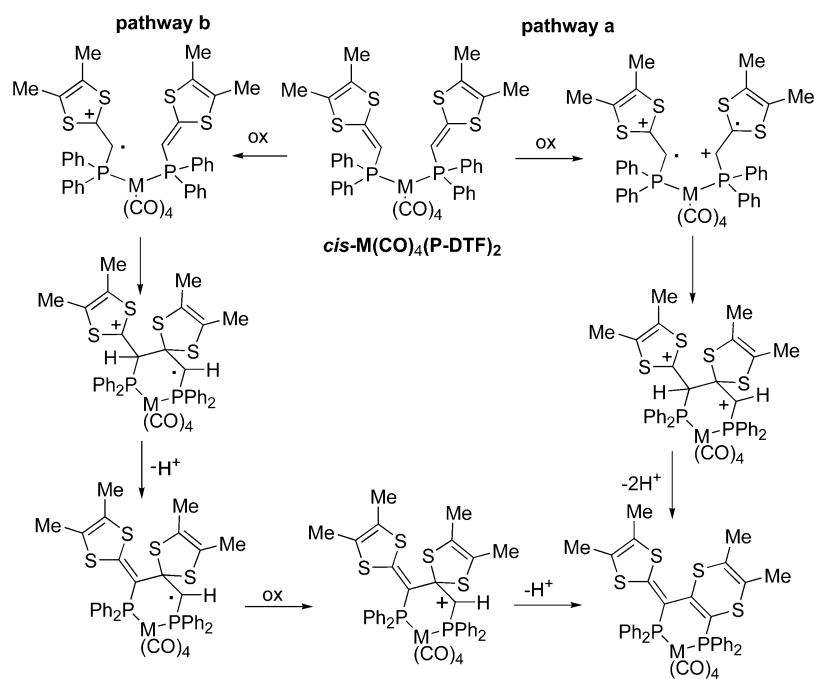
molecule A		molecule B	
Mo1–C102	1.981(5)	Mo2–C202	1.977(5)
Mo1–C104	1.985(6)	Mo2–C203	1.993(6)
Mo1–C103	2.029(5)	Mo2–C204	2.029(6)
Mo1–C101	2.037(5)	Mo2–C201	2.043(7)
Mo1–P101	2.5291(12)	Mo2–P202	2.5048(14)
Mo1–P102	2.5331(14)	Mo2–P201	2.5479(16)
P101–C105	1.842(4)	P201–C205	1.851(4)
P102–C107	1.831(4)	P202–C207	1.820(4)
S101–C105	1.762(4)	S201–C208	1.744(5)
S102–C106	1.788(4)	S202–C208	1.767(5)
S103–C108	1.761(4)	S203–C206	1.787(4)
S104–C108	1.753(4)	S204–C205	1.765(5)
C105–C106	1.341(6)	C205–C206	1.339(6)
C106–C107	1.483(5)	C206–C207	1.501(6)
C107–C108	1.361(5)	C207–C208	1.359(6)
P101–Mo1–P102	84.32(4)	P202–Mo2–P201	87.29(4)
C105–P101–Mo1	107.78(13)	C205–P201–Mo2	116.70(14)
C107–P102–C141	105.15(18)	C207–P202–C241	105.5(2)
C107–P102–C151	100.63(18)	C207–P202–C251	104.0(2)
C141–P102–C151	103.80(19)	C241–P202–C251	98.8(2)
C107–P102–Mo1	116.55(14)	C207–P202–Mo2	107.44(14)
C106–C105–S101	120.4(3)	C206–C205–S204	119.8(3)
C106–C105–P101	122.5(3)	C206–C205–P201	120.7(3)
S101–C105–P101	116.5(3)	S204–C205–P201	119.0(2)
C105–C106–C107	126.2(4)	C205–C206–C207	123.3(4)
C105–C106–S102	118.1(3)	C205–C206S203	119.2(4)
C107–C106–S102	115.4(3)	C207–C206–S203	116.9(3)
C108–C107–C106	118.6(3)	C208–C207–C206	116.5(4)
C108–C107–P102	127.1(3)	C208–C207–P202	125.3(4)
C106–C107–P102	113.7(3)	C206–C207–P202	116.0(3)
C107–C108–S104	128.3(3)	C207–C208–S201	128.4(4)
C107–C108–S103	120.4(3)	C207–C208–S202	119.9(4)
S104–C108–S103	111.3(2)	S201C208S202	111.6(2)

reaction,<sup>21</sup> but in this case mainly phosphine oxide was obtained due to the decomplexation of the vinylphosphine **2** from its metal complex. While replacing (BrC<sub>6</sub>H<sub>4</sub>)<sub>3</sub>NSbCl<sub>6</sub> by AgBF<sub>4</sub> we noticed an improvement of the yield of formation of the metallacycles, from 25% to 38% for the molybdenum and from 15% to 30% for the tungsten one. In both cases, together with the metallacycle we also obtained the mono(dithiafulvenyl) pentacarbonyl derivative, M(CO)<sub>5</sub>-

(20) Bellec, N.; Boubekeur, K.; Carlier, R.; Hapiot, P.; Lorcy, D.; Tallec, A. *J. Phys. Chem. A* **2000**, *104*, 9750.

(21) (a) Müller, H.; Salhi, F.; Divisia-Blohorn, B. *Tetrahedron Lett.* **1997**, *38*, 3215. (b) Lorcy, D.; Rault-Berthelot, J.; Poriel, C. *Electrochem. Commun.* **2000**, *2/6*, 382.

Scheme 6



(P-DTF). In the search for another better oxidizing agent, we also used 2,3-dichloro-5,6-dicyano-1,4-benzoquinone (DDQ). Actually, using this reactant, we did not observe the formation of the expected five-membered metallacyclic ring. Indeed, analysis of the reaction product by  $^{31}\text{P}$  NMR reveals an AX pattern, at  $\delta$  44.2 and 59.5 ppm with a  $^2J(\text{P,P})$  of 25 Hz for the molybdenum derivative and at  $\delta$  26.7 and 45.6 ppm with a  $^2J(\text{P,P})$  of 20 Hz for the tungsten derivative, indicating that the two phosphorus atoms are this time in nonequivalent environments. Similarly,  $^1\text{H}$  NMR spectra reveal a dissymmetrical structure with the disappearance of the vinylogous protons while mass spectrometry gave a composition similar to the one obtained for the five-membered metallacycles indicating that herein a coupling reaction also occurred. Single-crystal X-ray structure determination provided conclusive structural characterization of these metallacycles, where the coupling reaction upon oxidation with DDQ yield novel six-membered metallacycles **6** (Mo) and **7** (W) (Scheme 5 and Figure 4).

The molecular structure of **6** was established by X-ray diffraction (Figure 4), and selected bond distances and angles are given in Table 4. Two different molecules, **A** and **B**, are present in the asymmetric unit. In both molecules the metallacycle adopts a boat conformation with the C bearing the dithiole unit and the P atom above the plane. In molecule **A**, the folded 1,4-dithiine unit is oriented at the opposite direction of the dithiole while in the same direction for molecule **B**. The redox behavior of **6** and **7** was investigated by cyclic voltammetry in dichloromethane. For these metallacycles, only one irreversible oxidation wave was observed at  $E_{\text{pa}} = 0.70$  V for **6** and  $E_{\text{pa}} = 0.71$  V vs SCE for **7**.

It is worth noting that using DDQ as the oxidant the formation of the 1,4-dithiine ring is favored while with  $(\text{BrC}_6\text{H}_4)_3\text{NSbCl}_6$  or  $\text{AgBF}_4$  the expected vinylogous TTF core is formed. Thus, the strength of the oxidant,  $(\text{BrC}_6\text{H}_4)_3\text{NSbCl}_6 > \text{DDQ} > \text{AgBF}_4$ ,

does not appear to be the pertinent parameter for controlling the formation of either the five- or the six-membered metallacycle. At this stage we do not have any explanation for this different behavior. Nevertheless, two plausible mechanisms can be envisioned for the formation of **6** and **7**. As described in the Scheme 6 pathway a, DDQ ( $E^1 = 0.57$  V vs SCE in  $\text{CH}_2\text{Cl}_2$ ) can oxidize the two dithiafulvene cores into the bis cation radical, where one radical would be located on the dithiole ring; the coupling reaction would involve the formation of the six-membered metallacycle followed by the rearrangement and the deprotonation leading to the formation of the dithiine ring. The second pathway, pathway b, would involve first the oxidation of one dithiafulvene followed by the intramolecular cyclization with release of  $\text{H}^+$  leading to the six-membered metallacycle, which is further oxidized and rearranged into the dithiine followed by the deprotonation. Actually, this unusual rearrangement was rarely observed apart from 1,2-bis(1,4-dithiafulven-6-yl)benzene using  $\text{Br}_2$  as the oxidizing agent.<sup>22</sup>

## Conclusions

The coordinating ability of the dithiafulvenyl phosphine ligand toward the tungsten carbonyl fragment  $\text{W(CO)}_4$  has been investigated, and we have shown that it could behave as a monodentate (P) ligand or unexpectedly as a bidentate (P,S) ligand. Upon oxidation the formation of the vinylogous TTF core occurs in the coordination sphere of the  $\text{W(CO)}_4$  fragment, as also observed for the Mo analogue. Through the simple change of oxidizing agent, the carbon-carbon bond formation occurring upon oxidation of  $\text{cis-M(CO)}_4\text{-}$

(22) Lakshmikantham, M. V.; Cava, M. P.; Carroll, P. J. *J. Org. Chem.* **1984**, *49*, 726. (b) Frère, P.; Gorgues, A.; Jubault, M.; Riou, A.; Gouriou, Y.; Roncali, J. *Tetrahedron Lett.* **1994**, *35*, 1991.



*Dithiafulvenyldiphenylphosphine as a Ligand*

(P-DTF)<sub>2</sub> can be altered. Although the formation of the dithiine ring has been noted previously, at this stage no deductions could be drawn concerning what might drive the formation of either the five-membered or the six-membered metallacycle ring. Future investigations on this novel model of vinylogous tetrathiafulvalene complex will also focus on the nature of the molecular movement triggered by electron transfer.

**Note Added after ASAP:** This article was published ASAP on April 8, 2005, with a minor error in Scheme 6. The Web version published on April 11, 2005, and the print version are correct.

**Supporting Information Available:** X-ray crystallographic files in CIF format for complexes **3–6**. This material is available free of charge via the Internet at <http://pubs.acs.org>.  
IC0501465